

2D ECE-Imaging measurements of Edge Localised Modes (ELMs) at ASDEX Upgrade

J.E. Boom^{1*}, I.G.J. Classen^{2,1}, P.C. de Vries¹, W. Suttrop², T. Eich², N.K. Hicks², E. Wolfrum², R. Wenninger³, B.J. Tobias⁴, C.W. Domier⁴, N.C. Luhmann Jr.⁴, H.K. Park⁵, and the ASDEX Upgrade Team

¹*FOM Institute for Plasma Physics Rijnhuizen, 3430 BE Nieuwegein, the Netherlands*

²*Max-Planck-Institute für Plasmaphysik, 85748 Garching bei München, Germany*

³*Universitätssternwarte der Ludwig-Maximilians-Universität, 81679 München, Germany*

⁴*University of California at Davis, Davis, CA 95616, USA*

⁵*POSTECH, Pohang, Gyeongbuk, 790-784, Korea*

* E-mail: J.E.Boom@rijnhuizen.nl

Introduction

Due to steep pressure gradients at the plasma edge (in combination with high current densities), tokamak operation in high confinement mode is coupled to the occurrence of instabilities known as Edge Localised Modes (ELMs). In future fusion devices such as ITER, the heat load of particles expelled during these periodic relaxations of the edge barrier could prove difficult to handle [1].

There are still open questions concerning the dynamics of ELMs, particularly regarding their trigger mechanism, their spatial structure and the role of filaments with respect to particle and heat losses [2]. The installation in 2009 [3], [4] of an Electron Cyclotron Emission Imaging diagnostic (ECEI) on ASDEX-Upgrade (AUG) provides a new means to observe the nature of ELM crashes in 2D.

In this contribution, first the ECEI-system is shortly described and then measurements of different phases during a type-I ELM crash are presented, along with a first analysis of the mode that is observed at the onset of the crash.

ECE-Imaging at the plasma edge

The installed ECEI diagnostic consists of an array of 16 detectors, each of which acts as standard 1D ECE radiometer: it measures the intensity of the emitted radiation, here in 2nd harmonic X-mode, which is equal to intensity emitted by a black body at (electron) temperature T_e provided the plasma is optically thick. The quasi-optical setup allows for the 16 lines of sight (LOS) to be focussed at the low field side edge with spot sizes of 1.5 cm. The radial coverage is determined by 8 frequency bands per LOS, with inter-channel spacings of 800 MHz corresponding to 1.2 cm in the plasma. In total, this matrix of 16x8 channels covers an observation area of about 40x10 cm. Fig. 1(a) shows its location in a poloidal cross-section of AUG, which has minor horizontal and vertical radii of 0.5 m and 0.8 m; and in Fig. 1(b) the accompanying T_e profile (L-mode) of the central LOS is shown. Furthermore, ECEI is capable of measuring with a sampling rate up to 2 MHz.

Even though ECEI is not absolutely calibrated, electron temperatures can be obtained by cross-calibrating on the 1D-ECE diagnostic, which shares the same viewing window. Since in some cases there are channels lying outside the separatrix (normalised radius $\rho > 1$), an ‘intra-LOS’ calibration method has been used: first, the dependencies between all eight channels in each LOS are fixed (based on discharges at other magnetic fields where all channels are inside the separatrix). Then, for the desired case, only those channels that lie inside the separatrix are cross-calibrated and the others follow from the previously obtained dependencies. Fig. 1(b) and (c) respectively show the resulting T_e profiles, together with those from 1D-ECE, for typical L- and H-modes.

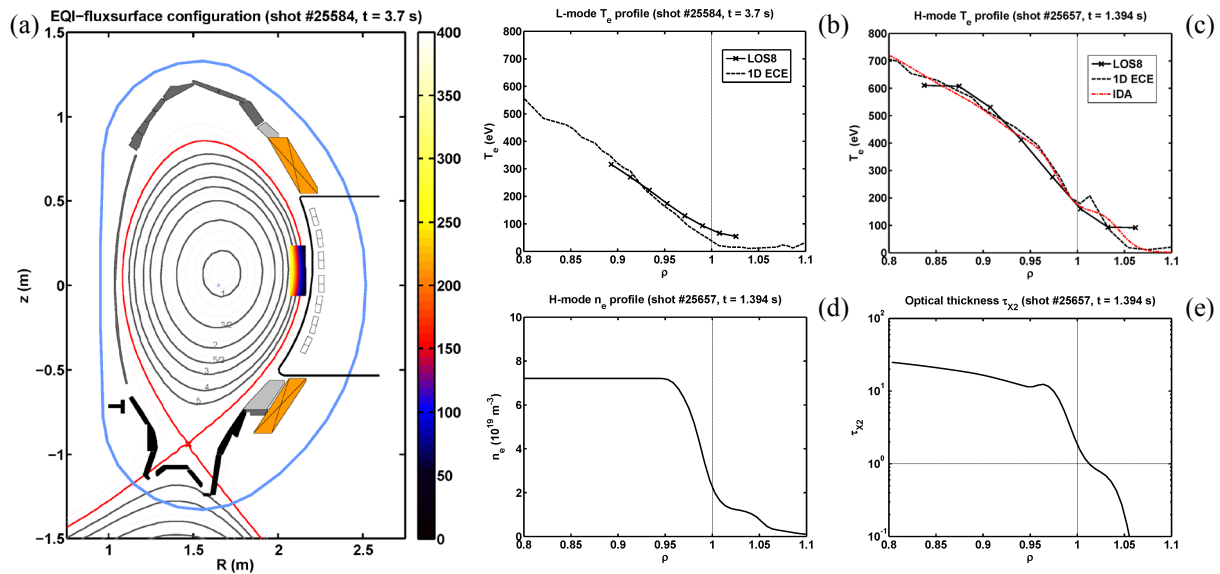


Fig. 1 The ECE-Imaging observational area for edge measurements is shown in (a), with the accompanying T_e profile (L-mode) for the central LOS in (b). In (c), T_e profiles are shown for an H-mode measured by both 1D ECE and ECEI, as well as an estimated profile from IDA. From the combination of T_e and the n_e profile shown in (d), the optical thickness is calculated as shown in (e).

In order to be able to interpret ECE radiation measurements at the edge (where T_e and electron density n_e have steep gradients) in terms of T_e , the optical thickness of the plasma should be sufficiently high. Based on the T_e and n_e profiles from Fig. 1(c) and (d), the optical thickness τ_{X2} is calculated as shown in Fig. 1(e). Here, integrated data analysis (IDA) [5] has been used to get values outside the separatrix as well, combining measurements from the lithium beam, DCN interferometer, and ECE (for T_e). Inside the separatrix $\tau_{X2} \gg 1$, so T_{rad} can safely be identified with T_e , which holds for standard H-mode discharges. Outside the separatrix in the region $1 < \rho < 1.03$, τ_{X2} drops below 1 making the plasma optically thin. Note that a slight increase of T_e and/or n_e could make the plasma optically thick again in this region, albeit marginally so interpretation should be done with care. For $\rho > 1.03$, τ_{X2} is so rapidly decreasing that T_{rad} can no longer be interpreted in terms of T_e .

2D ECE-Imaging measurements of a single ELM crash

With the ECEI observational area positioned at the low field side (LFS) plasma edge, and being aware of the described optical thickness difficulties, T_e measurements of ELMs can be made in 2D. Fig. 2 gives an overview of the (edge) plasma parameters of the H-mode discharge (#24793) where the measurements shown in Fig. 3 were made. The plasma current is 1.0 MA, the magnetic field 2.5 T, the edge safety factor q_{95} is 4.7, and T_e and T_i at the edge are about 500 and 700 eV. The line-averaged n_e is $8 \cdot 10^{19} \text{ m}^{-3}$ and near the edge it is $6 \cdot 10^{19} \text{ m}^{-3}$. The input power is 7 MW from NBI, and 750 kW from ECRH. As determined from the divertor current ($I_{\text{div.}}$) measurement, the ELM frequency is 80 Hz at the time of the measurement.

Different phases of the observed ELM crash are shown in Fig. 3. In (a), two T_e time-traces over more than a full ELM-cycle are shown; one of a channel inside and one just outside the separatrix (based on an equilibrium from before the crash). For

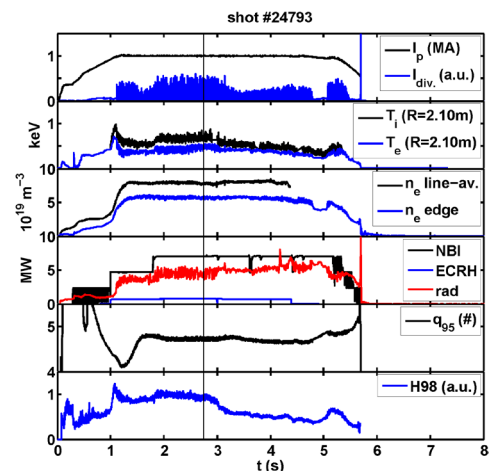


Fig. 2 The main discharge parameters of shot #24793, and indicated the time of the measurements of Fig. 3.

this example, it can be seen that the temperature collapse phase lasts 1.2 ms. In Fig. 3(b), first the T_e profile just before the crash is shown, and in (c) and (d) two images taken during the onset of the crash which show deformation of the profile inside the separatrix due to mode activity. The phase where the deformation shows a coherent poloidal mode structure lasts 65 μ s. The observed mode has a poloidal wavelength of ca. 15 cm, a displacement of almost 3 cm, and rotates with a poloidal velocity of 10 km/s in the electron magnetic drift direction (i.e. upward in the measurement's frame of reference). Within a couple of microseconds this then develops into rather complicated and incoherent structures starting the phase where the temperature begins to collapse.

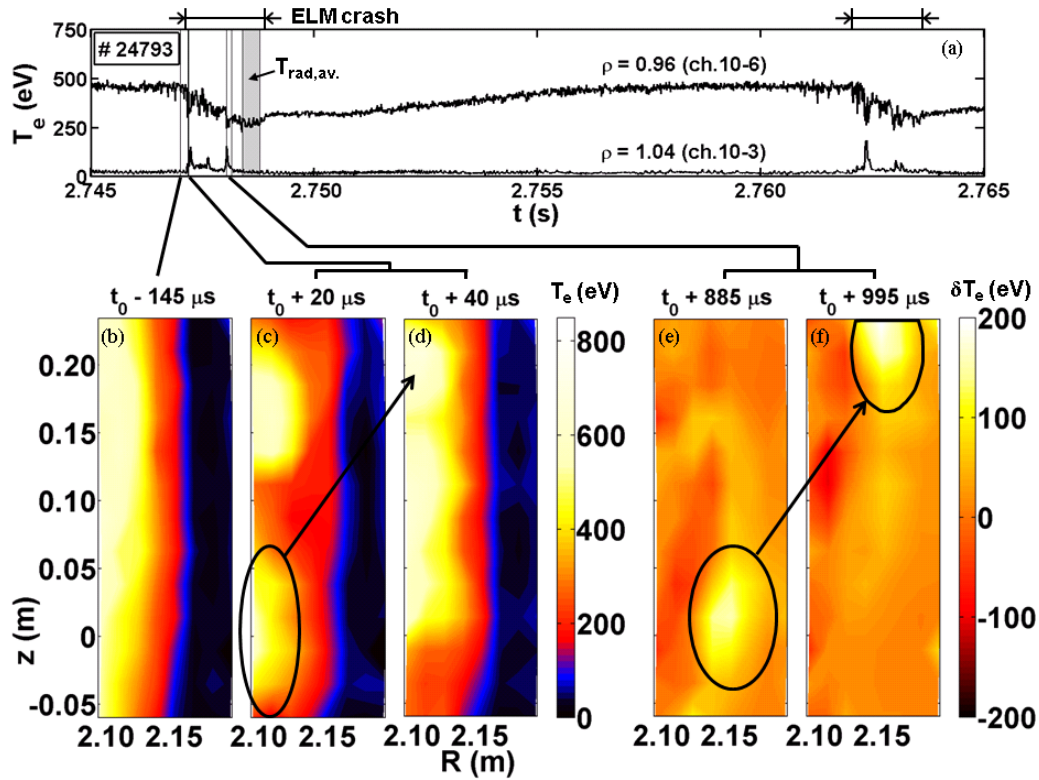


Fig. 3 The time trace in (a) shows the full ELM cycle. The stills in (b)-(f) respectively show a quiet phase just before the crash, two measurements at the onset of the temperature collapse phase, and the movement of poloidally localised structure of increased temperature a in the last two images (for which $T_{rad,av}$ is subtracted). The time t_0 marks the end of the quiet phase.

The measurements shown in Fig. 3(e) and (f) are taken towards the end of the temperature collapse phase and show a poloidally localised structure (≈ 7 cm) of increased local temperature around the very edge, rotating in the upward direction with a velocity of ca. 2 km/s. In order to enhance this structure, the images show $T_{rad} - T_{rad,av}$ rather than the absolute temperature; here, $T_{rad,av}$ is the average radiation temperature at the end of the crash (as indicated in Fig. 3(a)). Although the measurements were done in the region just outside the separatrix, the radiation temperatures (with maxima up to 200 eV) can most likely still be interpreted in terms of electron temperature. This is assuming that, with locally increased electron densities, the optical thickness inside the structure could (marginally) be above 1.

Mode analysis

A first step in the analysis of the ECEI measurements, in order to make comparisons to other diagnostics or to results from modelling, is to determine the mode number of mode observed at the onset of the temperature collapse phase. For this purpose, a second example of a mode (seen at the onset of another crash) is shown in Fig. 4; with discharge #24841 having the same plasma parameters as #24793 (cf. Fig. 2).

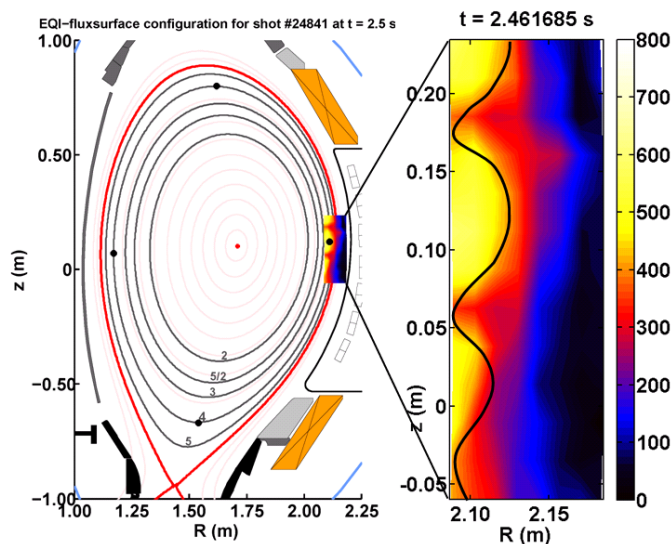


Fig. 4 Second example of a mode observed at the onset of an ELM crash. On the left, the fluxsurface configuration at the time of the crash is shown; the image on the right shows the mode structure magnified (indicated by a line to guide the eye).

of the $q = 4$ surface) and is 9 cm. The circumference of the $q = 4$ surface can be approximated by an ellipse going through the four dots indicated in the left graph of Fig. 4, and is estimated to be 3.83 m. It then follows that the poloidal mode number m of the observed mode is 43, which at the $q = 4$ surface corresponds to a toroidal mode number n of about 11. For comparison, the same analysis is applied to the mode shown in Fig. 3(c) and the resulting toroidal mode number n is 8.

Discussion and outlook

Concerning the modes at the ELM onset as shown here, the estimated mode numbers are in the ball park of what has been commonly observed at AUG [6], [7]. It must however be noted that these modes are not seen by ECEI in every ELM crash, which might be explained e.g. by a toroidally localised onset of the ELM. Secondly, the spatial resolution of ECEI will limit the measurements to maximally resolve poloidal m numbers of about 160. Furthermore, the method used here also needs to be evaluated to one using a straight field line angle approach.

As to the poloidally localised structures of increased temperature, taking into account that interpretation of ECE measurements (just) outside the plasma edge is not straightforward, they are thought to be related to so called filaments which are observed by other diagnostics as well [7].

The next steps in this research will be to compare the observed modes to JOREK calculations [2], and to try and find on what plasma parameters their properties depend. Additionally, regarding the filaments, a comparison will be made to soft X-ray measurements in order to reveal more detail on the direction of movement of these structures.

References

- [1] G. Federici et al., Plasma Phys. Control. Fusion 45 (2003) 1523
- [2] G.T.A. Huysmans and O. Czarny, Nucl. Fusion 47 (2007) 659
- [3] I.G.J. Classen et al., Rev. Sci. Instrum. (2010) tbp
- [4] I.G.J. Classen et al., this conference (P-4.182)
- [5] R. Fischer et al., 36th EPS Conference on Plasma Phys. (2009) ECA Vol.33E, P-1.159
- [6] Kirk A et al., J. Phys.: Conf. Ser. 123 (2008) 012011
- [7] T. Eich et al., Plasma Phys. Control. Fusion 47 (2005) 815

A rough approximation for the poloidal mode number m can be determined as follows: as the left graph in Fig. 4 shows, the mode is located on the $q = 4$ surface. From the right graph in Fig. 4, the poloidal wavelength of the mode is estimated to be 11.5 cm on the low field side. Assuming Liouville's theorem is applicable (i.e. constant phase-space distribution over the whole trajectory of the mode), the poloidal wavelength of the mode varies with the magnetic field over the fluxsurface and it is largest on the LFS and smallest on the high field side. Since the magnetic field is mainly dependent on major radius R , the average poloidal wavelength follows from the ratio of R_{LFS} and R_{av} (taken at the top